Journal of Cellular Biochemistry 97:178–187 (2006)

Prevention of Geranylgeranoic Acid-Induced Apoptosis by Phospholipid Hydroperoxide Glutathione Peroxidase Gene

Yoshihiro Shidoji,[1]* Kyoko Okamoto,[1] Yasutoshi Muto,[2] Sadaaki Komura,[3] Nobuko Ohishi,[3] and Kunio Yagi[3]

[1]Molecular and Cellular Biology, Graduate School of Human Health Sciences, Siebold University of Nagasaki, Nagayo, Nagasaki 851-2195, Japan
[2]Gifu University School of Medicine, Gifu, Gifu 500-8705, Japan
[3]Institute of Applied Biochemistry, Mitake, Gifu 505-0116, Japan

Abstract Micromolar concentrations (0.5 ~ 5 μM) of all-*trans* geranylgeranoic acid (GGA) induced cell death in a guinea pig cell line, 104C1, whereas under the same conditions GGA was unable to kill 104C1/O4C, a clone established from 104C1 cells by transfection of them with the human phospholipid hydroperoxide glutathione peroxidase (*PHGPx*) gene. GGA (5 μM) induced a loss of the mitochondrial inner membrane potential ($\Delta\Psi$m) in 104C1 cells in 2 h, and their apoptotic cell death became evident in 6 h. On the other hand, 104C1/O4C cells were resistant to loss of $\Delta\Psi$m and showed intact morphology until at least 24 h after addition of 10 μM GGA. Dihydroethidine, superoxide-sensitive probe, was immediately oxidized 15 min after addition of GGA in both 104C1 and 104C1/O4C cells. The peroxide-sensitive probe 2′,7′-dichlorofluorescin diacetate (H_2-DCF-DA) was strongly oxidized in 104C1 cells 4 h after the addition of 2.5 μM GGA, but not in 104C1/O4C cells even in the presence of 10 μM GGA. The present results suggest that GGA induced a hyper-production of superoxide and subsequently peroxides, which in turn may have led to dissipation of the $\Delta\Psi$m and final apoptotic cell death in 104C1 cells. J. Cell. Biochem. 97: 178–187, 2006.

Key words: geranylgeranoic acid; mitochondrial inner membrane potential; reactive oxygen species; phospholipid hydroperoxide glutathione peroxidase; apoptosis

All-*trans* geranylgeranoic acid (GGA) has been reported as a micromolar lipid inducer of differentiation and/or apoptosis in the human hepatoma-derived cell line HuH-7 [Yamada et al., 1994; Nakamura et al., 1995] as well as a potent ligand for both cellular retinoic acid-binding protein [Muto et al., 1981] and nuclear retinoid receptors [Araki et al., 1995]. The induction of hepatic differentiation in HuH-7 cells by GGA derivatives (e.g., 4,5-didehydro GGA), as evidenced by up-regulation of albumin production and hepatocyte nuclear factor-1 gene expression and down-regulation of α-fetoprotein and c-myc gene expression can be explained by their retinoidal action through transacting factors, i.e., retinoic acid receptors (RARs) and retinoid X-activated receptors (RXRs). Because 9-*cis* retinoic acid, a putative natural ligand for both RAR and RXR, showed the same effects at its sub-micromolar concentration on the cellular expression of the above-mentioned genes as 4,5-didehydro GGA did at higher (micromolar) concentrations [Yamada et al., 1994], GGA and 4,5-didehydro GGA have been recognized acyclic retinoids that show rather weaker potency to transactivate their target genes than natural retinoids [Araki et al., 1995].

In contrast, its apoptosis-inducing ability seems to be a non-retinoidal function of GGA, because neither all-*trans* nor 9-*cis* retinoic acid caused the death of the hepatoma cells [Nakamura et al., 1995]. Interestingly, this extra-retinoid function of GGA was found

Kunio Yagi has deceased.

*Correspondence to: Dr. Yoshihiro Shidoji, Molecular and Cellular Biology, Graduate School of Human Health Sciences, Siebold University of Nagasaki, Academy Hills 1-1-1, Nagayo, Nagasaki 851-2195 Japan.
E-mail: shidoji@sun.ac.jp

Received 19 May 2005; Accepted 25 July 2005
DOI 10.1002/jcb.20627

selectively in hepatoma cells but not in primary hepatocytes [Nakamura et al., 1996; Shidoji et al., 1997]. Although the molecular mechanism of GGA-induced apoptosis has proved to be elusive, the hepatoma-selective induction of apoptosis by GGA apparently coincides with GGA-induced dissipation of the mitochondrial inner membrane potential ($\Delta\Psi m$) [Shidoji et al., 1997]. α-Tocopherol, a lipophilic antioxidant, substantially protected mitochondria from the rapid collapse of $\Delta\Psi m$ and blocked the apoptotic cell death until 24 h after addition of GGA [Shidoji et al., 1997], suggesting that the GGA-induced loss of $\Delta\Psi m$ may be conveyed by excessive oxidation reactions in the vicinity of the mitochondrial inner membrane.

Recently, we found that transfection of guinea pig cells with human phospholipid hydroperoxide glutathione peroxidase (PHGPx) cDNA [Esworthy et al., 1994] carrying a code for a mitochondrial-transfer signal protected the cells from lipid hydroperoxide-mediated cell injury by preventing the dissipation of the $\Delta\Psi m$ [Yagi et al., 1996, 1998]. It has been suggested that mitochondrial PHGPx plays a preventive role against hydroperoxide-mediated injury to mitochondria by enzymatically reducing hydroperoxides of cardiolipin, a peculiar phospholipids abundant in the mitochondrial inner membrane [Duan et al., 1988; Sun et al., 1997]. Cardiolipin is particularly rich in polyunsaturated fatty acids, which are vulnerable to oxidative attack. It is reasonable to think that mitochondrial cardiolipin may be degraded by enhanced peroxidation reactions during apoptotic cell death. In fact, Vogelstein's group reported a dramatic decrease in the intracellular content of mitochondrial cardiolipin soon after reactive oxygen species (ROS) had been generated during p53-induced apoptosis [Polyak et al., 1977]. Hence, one can speculate that PHGPx may hamper the mitochondrial damage and cell death induced by GGA.

In the present study, we addressed whether GGA could enhance peroxidation reactions in guinea pig cells and whether the human *PHGPx* or *hGPX-4* gene would be able to prevent GGA-induced disruption of $\Delta\Psi m$ and to block the resultant apoptotic cell death. By using several fluorogenic probes sensitive to either $\Delta\Psi m$ or intracellular peroxidation reactions, we found that micromolar concentrations of GGA induced a rapid loss of $\Delta\Psi m$ in the guinea pig cells and that the ectopic and constitutive expression of the *hGPX-4* gene prevented the early collapse of $\Delta\Psi m$, which prevention coincided with a reduction in the level of intracellular peroxide.

MATERIALS AND METHODS

Materials

The guinea pig cell line used, 104C1, an in vitro transformed fibroblast-derived cell line, was obtained from the Japanese Cancer Research Resources Bank (Tsukuba, Japan). 104C1/O4C, a stable transfectant clone constitutively expressing the *hGPX-4* gene, was established from 104C1 by us as described in detail previously [Yagi et al., 1996]. A $\Delta\Psi m$-sensitive fluorescent probe, JC-1 (5,5′,6,6′-tetrachloro-1,1′,3,3′-tetraethyl-benzimidazolylcarbocyanine iodide) was purchased from Molecular Probes (Eugene, OR). A fluorophore specific for peroxidation reactions, 2′,7′-dichlorofluorescin diacetate (H_2-DCF-DA) [Afri et al., 2004] was from Kodak (Rochester, NY). Dihydroethidine, a fluorogenic probe for superoxide-mediated reactions [Daiber et al., 2004], was obtained from Sigma-Aldrich (Tokyo, Japan). All-*trans* GGA was kindly provided by Kuraray Co. (Kurashiki Okayama, Japan).

Treatment of Cells With GGA

Cells from confluent cultures of 104C1 or 104C1/O4C cells were inoculated into 12-well culture plates after a 12-fold dilution with RPMI 1640 medium (Sigma-Aldrich) containing 10% fetal bovine serum (FBS). Two days before the treatment of cells with GGA, the medium was replaced with FBS-free RPMI 1640. The ethanolic solution of GGA (10 mM) was added to the medium at the final concentrations indicated in the legends of Figures. The concentration of the vehicle in the medium was adjusted to 0.1 (v/v)%.

Fluorescence Microscopy

After the addition of GGA, the $\Delta\Psi m$ was visualized by vital staining of mitochondria with 2 μg/ml JC-1. Its monomeric green fluorescence or J-aggregate-dependent red fluorescence was observed with a Nikon Diaphot-TMD inverted fluorescence microscope. The data for microscopic images were obtained by use of the NIH Image program (ver 1.62, developed at the U.S. National Institutes of Health, Bethesda, MD) to measure the cellular intensity of the red fluorescence as the integrated density per cell

by summing of the pixels in each cell with background subtracted and processing on a StatView, ver 4.5 to make histogram.

Intracellular peroxidation reactions were observed by fluorogenic conversion of either H_2-DCF-DA to 2′,7′-dichlorofluorescein (DCF) or dihydroethidine to ethidium. The cellular intensity of the yellow–green fluorescence of DCF in the cytoplasm and the red fluorescence of ethidium intercalated in the chromosomal DNA were calculated with the NIH Image software, the same as indicated above.

Others

A number of viable cells were counted on a Burker-Turk counter by Trypan blue dye-exclusion after detachment with trypsin. The concentration of GGA was measured by liquid chromatography-mass spectrometry (LC/MS) [Shidoji and Ogawa, 2004]. HPLC was performed by using a Waters 2690 separations module (Waters, Milford, MA) equipped with a semi-micro Capcell-Pak UG80 reverse-phase C-18 column (2.0 × 50 mm, 3 μm; Shiseido Fine Chemicals, Tokyo, Japan). In-line MS was performed by using a Waters ZMD 2000 equipped with an electrospray interface and operated in the negative ion mode.

RESULTS

GGA-Induced Cell Death in PHGPx-Null Cells, But Not in PHGPx-Expressing Cells (Fig. 1)

It is well established that guinea pig fibroblast-derived 104C1 cells produce no PHGPx enzyme [Yagi et al., 1996]. Figure 1 shows the effects of GGA treatment on the viability of PHGPx-negative (104C1) and -positive guinea pig cell lines (104C1/O4C). When 104C1 cells were exposed to 10 μM GGA, the cells started to die in 6 h, and almost all of them were gone in 24 h (Fig. 1A). In the dose-response experiment, at 16 h, the cells started to die at 2.5 μM GGA, almost all died at more than 20 μM GGA, and half of the cell population died at approximately 6.5 μM GGA (ld50) (Fig. 1B). The mode of the cell death was suggested to be apoptosis in view of the morphological changes such as chromatin condensation (data not shown). In sharp contrast, the 104C1/O4C cells, a 104C1-derived clone that constitutively expresses the *hGPX-4* gene and accumulates hPHGPx enzyme protein in its mitochondria [Yagi et al., 1996], survived and even grew well in the presence of 10 μM GGA (Fig. 1A) and were still alive at 16 h even at the maximum concentration tested, i.e., 50 μM GGA (Fig. 1B), indicating that the constitutive expression of the *hGPX-4* gene produced a new phenotype resistant against GGA.

GGA-Induced Collapse of ΔΨm in PHGPx-Null Cells, But Not in PHGPx-Expressing Cells (Fig. 2)

During GGA-induced apoptosis in human hepatoma-derived HuH-7 cells, we found immediate and dramatic changes in ΔΨm by using rhodamine 123 [Shidoji et al., 1997]. In the present study, ΔΨm was measured with the fluorogenic probe JC-1, which is a more quantitative indicator for ΔΨm than rhodamine 123. The red fluorescence of JC-1 was detected in the cytoplasmic space and was excluded from the nuclear region of 104C1 cells, although the

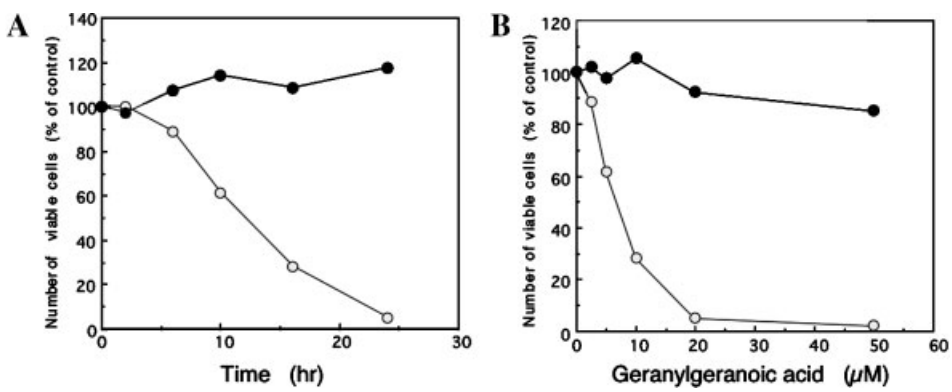

Fig. 1. Viable cell number after treatment of 104C1 (open circle) and 104C1/O4C (closed circle) cells with all-*trans* geranylgeranoic acid (GGA). **A**: Relative cell number is expressed as a percentage of the control (0–time cultures) at the indicated time points after addition of 10 μM GGA. Each point represents the mean value of triplicate wells. **B**: Relative cell number is expressed as a percentage of the control (vehicle-treated cultures) at 16 h after addition of GGA at the indicated concentrations. Each point represents the mean value of triplicate wells.

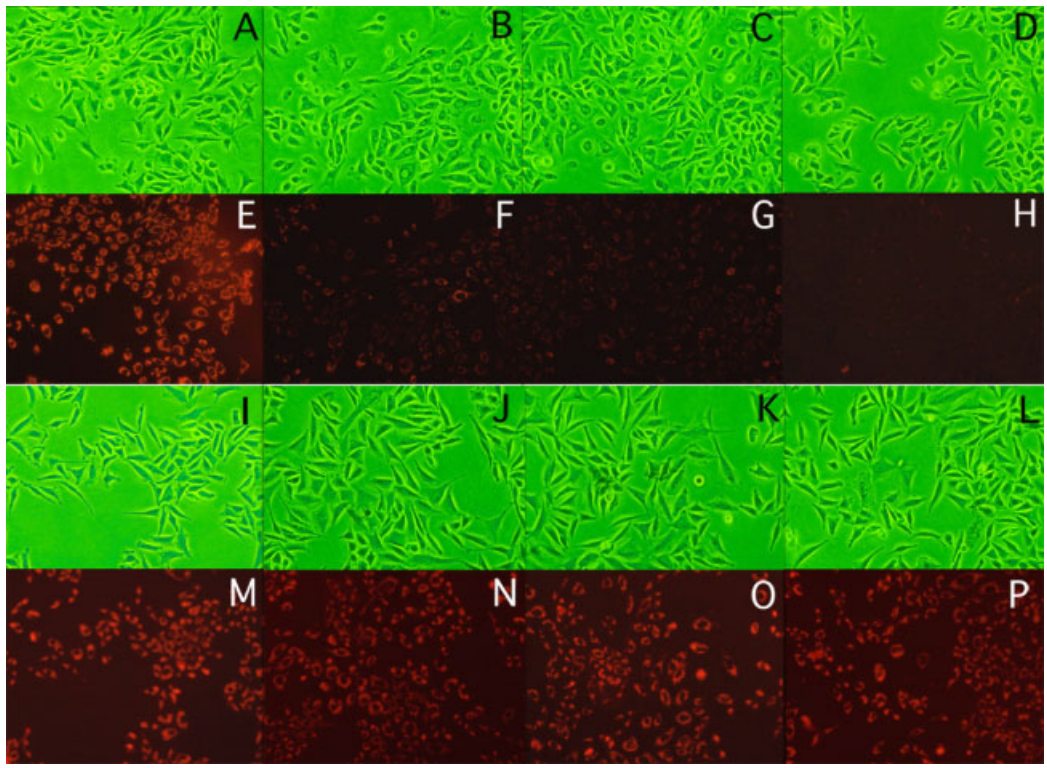

Fig. 2. Phase-contrast and JC-1 fluorescence micrographs of 104C1 (**upper two panels**) and 104C1/O4C (**lower two panels**) cells treated with different concentrations of GGA. 104C1 cells were treated with vehicle alone (**A**, **E**) or 0.5 (**B**, **F**), 1 (**C**, **G**), or 5 (**D**, **H**) μM GGA. The red fluorescence of JC-1 aggregates was detected at 2 h after addition of GGA (E–H), and phase-contrast micrographs of the same fields were also taken at the same time (A–D). 104C1/O4C cells were treated with vehicle alone (**I**, **M**) or 0.5 (**J**, **N**), 1 (**K**, **O**), or 5 (**L**, **P**) μM GGA. JC-1 aggregates, as indicated by the red fluorescence, were detected at 2 h after the addition of GGA (M–P). Corresponding phase-contrast micrographs were also taken at the same time (I–L). This experiment was conducted by using triplicate wells, and representative results are shown. [Color figure can be viewed in the online issue, which is available at www.interscience.wiley.com.]

intensity of cellular fluorescence was variable among cells depending on their $\Delta\Psi m$ (Fig. 2E). A rapid (2 h) and significant ($P < 0.005$) loss of $\Delta\Psi m$ was induced even at 0.5 μM GGA (Figs. 2F, 3B), without any morphological changes discernible by phase-contrast microscopy (Fig. 2B). The disruptive effect of GGA on $\Delta\Psi m$ was dose dependent in 104C1 cells (Figs. 2, 3). Under the basal condition, 104C1/O4C cells harboring the *hGPX-4* gene also showed the red fluorescence of JC-1 only in their cytoplasm (Fig. 2M). In sharp contrast to the parent 104C1 cells, however, the 104C1/O4C cells did not lose the cytoplasmic red fluorescence even in the presence of 5 μM GGA (Fig. 2P), indicating that the cells and their mitochondria became apparently resistant to the GGA treatment.

When these fluorescent images were quantitatively analyzed by NIH-Image software, the relative intensity of JC-1 red fluorescence per cell showed a normal distribution with the mean value of $41{,}750 \pm 1{,}750$ pixels/cell (mean ± SEM) in the vehicle-treated 104C1 cells (Fig. 3A). The mean cellular intensity of the red fluorescence was logarithmically decreased by increasing the concentration of GGA from 0.5 to 5 μM (Fig. 3A–D). On the other hand, the mean value of the cellular intensity of the red fluorescence was slightly increased in PHGPx-positive clonal 104C1/O4C cells, compared with that of the 104C1 cells under the basal condition. Furthermore, in sharp contrast to the case of 104C1 cells, increasing the concentration of GGA even to 5 μM failed to diminish the red fluorescence in these cells (Fig. 3H).

Hyper-Production of Peroxidation Reactions Induced by GGA in Both Cell Lines

Figure 4 shows the effects of increasing the concentration of GGA on the production of cellular ROS, as probed by dihydroethidine, in both cell lines. When dihydroethidine was oxidized by ROS such as superoxide anion radicals in the cells, the resultant ethidium became

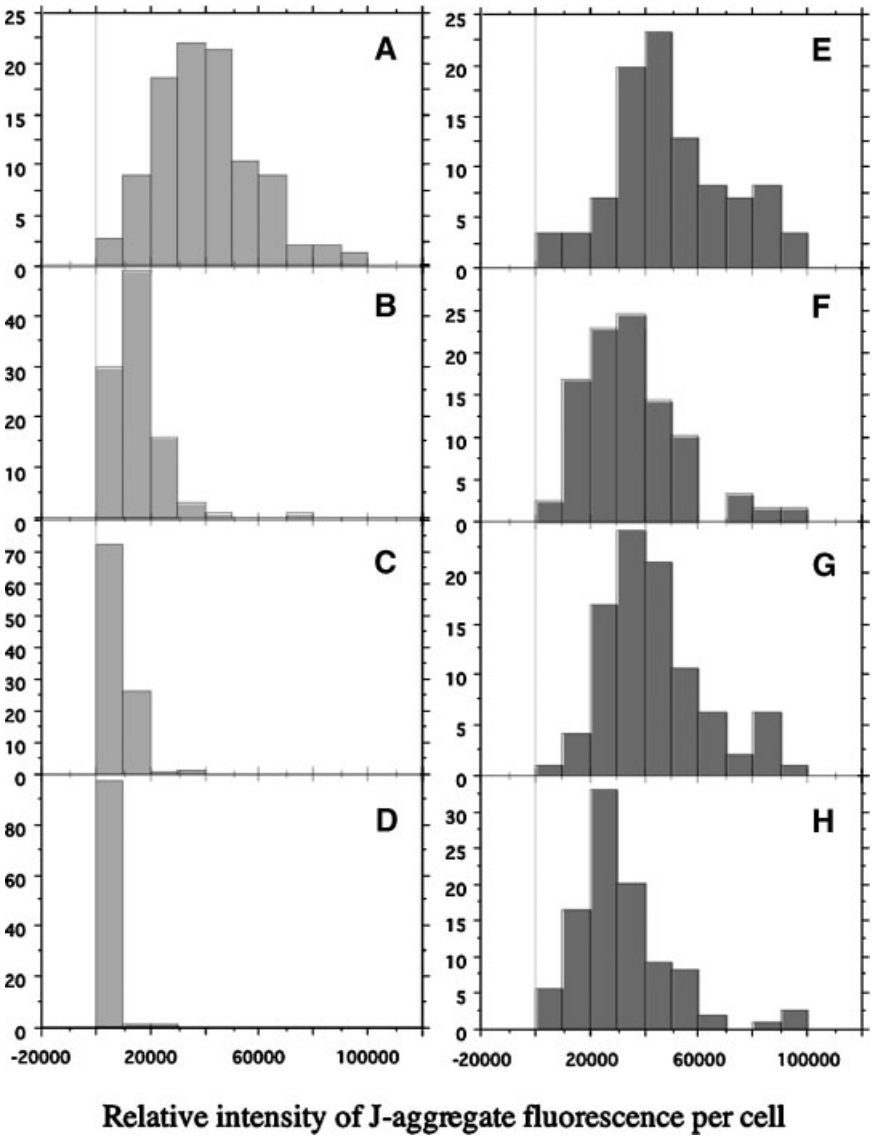

Fig. 3. Histograms of the intensity of cellular JC-1 red fluorescence in 104C1 (**left panels**) and 104C1/O4C (**right panels**) cells treated with different concentrations of GGA. From the results of the experiment shown in Figure 2, the fluorescence images were quantitatively analyzed as described in the ''Materials and Methods.'' The abscissa shows the relative intensity of JC-1 red fluorescence per cell, expressed as pixels/cell; and the ordinate, the percentage distribution of hierarchy. 104C1 cells were treated for 1 h with vehicle alone (**A**) or 0.5 (**B**), 1 (**C**) or 5 (**D**) μM GGA. The intensity of red fluorescence of JC-1 aggregates was quantified per cell basis, and the mean values with standard errors were 41.8 ± 1.8 (A), 14.5 ± 1.1 (B), 8.1 ± 0.45 (C), and 1.8 ± 0.4 (D) k pixels/cell. 104C1/O4C cells were treated for 1 h with vehicle alone (**E**) or 0.5 (**F**), 1 (**G**) or 5 (**H**) μM GGA. The intensity of red fluorescence of JC-1 aggregates was quantified as stated above, and the mean values with standard errors were 50.1 ± 2.5 (E), 38.0 ± 2.0 (F), 47.4 ± 2.5 (G), and 33.8 ± 2.1 (H) k pixels/cell.

intercalated into the genomic DNA, thus producing nuclei with red fluorescence. The oxidation reaction of dihydroethidine to the red-fluorescent ethidium was induced in 15 min after the addition of 0.5 μM GGA in both cell lines (Fig. 4F, N). Furthermore, both cell lines were similarly dose dependently sensitive to GGA from 0.5 to 5 μM to oxidize dihydroethidine. The time-course of GGA-induced oxidation of dihydroethidine was also similar in both cell lines, with a peak between 15 and 30 min after the addition of GGA, and the red fluorescence returned to the base line in 60 min (Fig. 5).

Next, we searched other ROSs such as peroxides to differentiate the effects of GGA in the PHGPx-negative and -positive cell lines. Until 2 h of GGA-treatment, GGA produced no change in the rate of oxidation of H_2-DCF-DA in

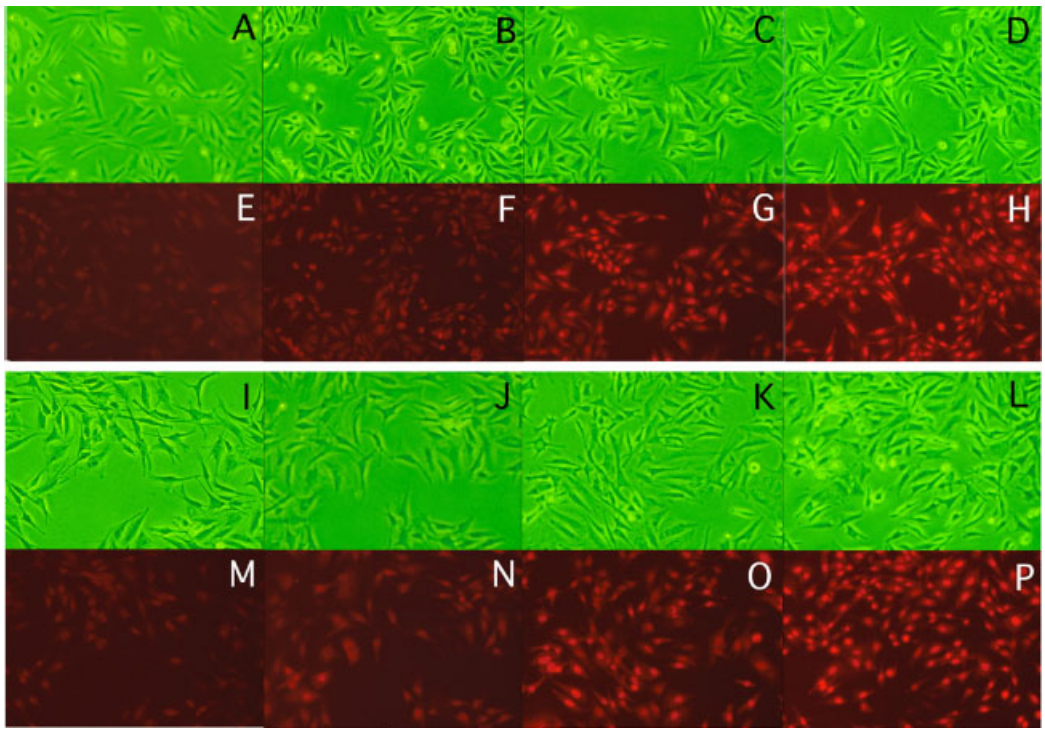

Fig. 4. Phase-contrast and dihydroethidine fluorescence micrographs of 104C1 (**upper two panels**) and 104C1/O4C (**lower two panels**) cells treated with different concentrations of GGA. 104C1 cells were treated with vehicle alone (**A**, **E**) or 0.5 (**B**, **F**), 1 (**C**, **G**) or 5 (**D**, **H**) μM GGA. The red fluorescence of ethidium intercalated into the nuclear DNA was detected at 15 min after the addition of GGA (E–H), and corresponding phase-contrast micrographs were also taken at the same time (A–D). 104C1/O4C cells were treated with vehicle alone (**I**, **M**) or 0.5 (**J**, **N**), 1 (**K**, **O**) or 5 (**L**, **P**) μM GGA. Ethidium was detected at 15 min after the addition of GGA (M–P), and respective phase-contrast micrographs were also taken at the same time (I–L). This experiment was conducted with triplicate wells, and representative results are shown. [Color figure can be viewed in the online issue, which is available at www.interscience.wiley.com.]

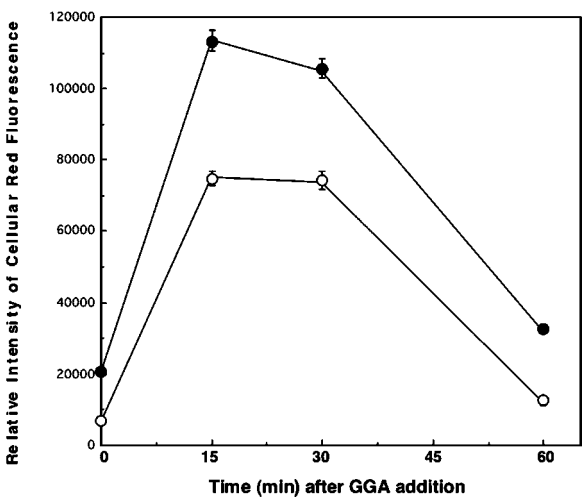

Fig. 5. Time-dependent changes in cellular intensity of dihydroethidine-derived red fluorescence of 104C1 (open circles) and 104C1/O4C (closed circles) cells treated with 5 μM GGA. The red fluorescence of ethidium intercalated into the nuclear DNA was quantitatively analyzed as described in the "Materials and Methods." Each point represents the mean ± SE ($n = 500 \sim 1{,}000$).

either cell line compared with the rate for the vehicle-treated cells (data not shown). A 4-h treatment of 104C1 cells with 2.5 μM GGA caused the intracellular production and accumulation of DCF, a green–yellow fluorescent and peroxidative product derived from the non-fluorescent H_2-DCF-DA (Fig. 6D). In contrast, the 104C1/O4C cells produced only small amount of the fluorescent product after a 4-h treatment with 5 μM GGA (Fig. 6H). When the fluorescent images were analyzed quantitatively by using the NIH-Image software, the basal production of peroxides in the PHGPx-positive cells was significantly less than that in the enzyme-negative cells, as shown in Figure 7. As a result, a ratio of DCF fluorescence intensity in 104C1 cells to that in 104C1/O4C cells was increased from 39.5 to 90.3 by the GGA treatment.

DISCUSSION

In the present study, we clearly showed for the first time that GGA at micromolar concen-

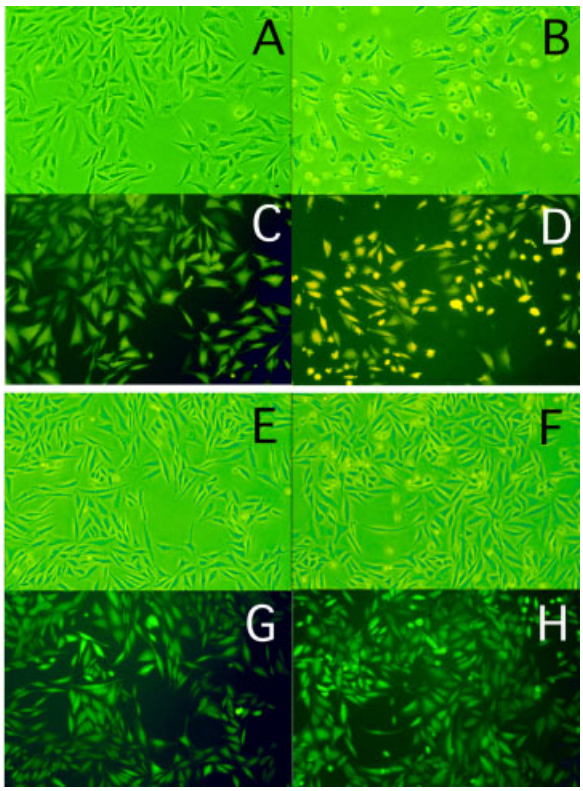

Fig. 6. Phase-contrast and 2′,7′-dichlorofluorescein (DCF) fluorescence micrographs of 104C1 (**upper four panels**) and 104C1/O4C (**lower four panels**) cells after treatment with GGA. 104C1 cells were treated with vehicle alone (**A**, **C**) or 2.5 μM GGA (**B**, **D**). The green–yellow fluorescence of DCF generated in the cytoplasm was detected at 4 h after the addition of GGA (C, D). Phase-contrast micrographs of the same fields were also taken at the same time (A, B). 104C1/O4C cells were treated with vehicle alone (**E**, **G**) or 2.5 μM GGA (**F**, **H**). DCF fluorescence was observed at 4 h after the addition of GGA (G, H), and corresponding phase-contrast micrographs were also taken at the same time (E, F). Triplicate wells were used, and representative results are shown. [Color figure can be viewed in the online issue, which is available at www.interscience.wiley.com.]

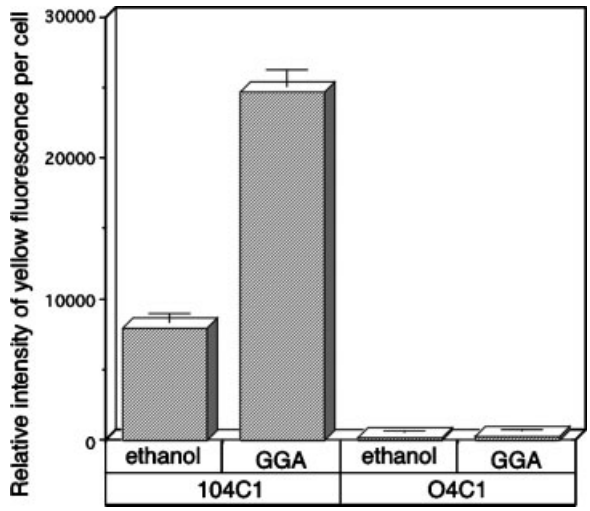

Fig. 7. Quantitative analysis of the intensity of cellular DCF green–yellow fluorescence in 104C1 and 104C1/O4C cells after treatment with GGA. From the results of the experiment shown in Figure 6, the fluorescent images were quantitatively analyzed as described in the ''Materials and Methods.'' Mean ± SE ($n = 500 \sim 1{,}000$).

trations induced a rapid loss of the mitochondrial inner membrane potential (ΔΨm) in 104C1 cells through hyper-production of ROS. In other words, the forced expression of the *hGPX-4* gene was unequivocally shown to cancel this early effect of the micromolar polyprenoic acid on the mitochondrial function. Consequently, GGA-resistance was established in these PHGPx-expressing cells.

Previously, we found a transient loss of ΔΨm during GGA-induced apoptosis in HuH-7 cells in the presence of caspase inhibitors [Shidoji et al., 1997]. These peptide inhibitors blocked or delayed the GGA-induced apoptotic cell death, but did not prevent the rapid loss of ΔΨm; and the dissipated ΔΨm was restored later to the normal level. Furthermore, α-tocopherol protected the mitochondria of hepatoma cells from the rapid collapse of ΔΨm as well as the cells from GGA-induced apoptotic cell death [Shidoji et al., 1997]. Therefore, we proposed that mitochondrial dysfunction (loss of ΔΨm) might be an early and triggering event for cell death, although the loss of ΔΨm was still a reversible process during the GGA-induced apoptosis. Although α-tocopherol is a well-known antioxidant, we were unaware which ROSs might be involved in the GGA-induced apoptosis, because α-tocopherol prevented GGA-induced hyper-production of both superoxide anion radicals and hydrogen peroxides probed by dihydroethidine and H_2-DCF-DA in HuH-7 cells, respectively (unpublished results).

Guinea pig-derived 104C1 cells are known to have a negligible level of endogenous PHGPx enzyme protein [Yagi et al., 1996], and the addition of selenium to the medium did not induce any activity of PHGPx [Sun et al., 1997]. PHGPx is a unique antioxidant enzyme in that it reduces lipid hydroperoxides and possesses an N-terminal mitochondrial targeting signal [Pushpa-Rekha et al., 1995]. One can well expect that phospholipid hydroperoxides, once formed intracellularly, might efficiently accumulate all over the membrane system, including the mitochondrial inner membrane, of the 104C1 cells. When the peroxidized lipid reaches

the inner membrane of mitochondria, the lipid might induce a permeability transition that could be involved in the collapse of the $\Delta\Psi m$ [Skulachev, 1996]. In fact, phosphatidylcholine monohydroperoxide, when added to the culture medium, caused a rapid and transient dissipation of the $\Delta\Psi m$ and apoptotic cell death in 104C1 cells, but not in 104C1/O4C cells [Yagi et al., 1998]. Because concrete evidence has accumulated indicating peroxidative modifications of mitochondrial proteins (e.g., adenine nucleotide translocase or ANT) and lipids (e.g., cardiolipin) in cell-free systems [Masini et al., 1993; Giron-Calle and Schmid, 1996; Ritov et al., 1996; Halestrap et al., 1997], we can easily assume that exogenous phospholipid hydroperoxides might cause oxidative damage to ANT and cardiolipin in the mitochondria of 104C1 cells. Similar disruption of intracellular processes may well happen in GGA-treated 104C1 cells. If ANT and cardiolipin are damaged by the peroxidation reactions induced by GGA treatment, it would be difficult for the cell to keep its $\Delta\Psi m$ intact.

It is worthwhile to mention that mitochondrial PHGPx is colocalized with ANT at the contact site between the inner- and outer-membranes, where other proteins are known to exist, such as cardiolipin synthetase, Bcl-2, porin, and so on [Kroemer et al., 1997], thus suggesting that PHGPx may be an active component of the permeability transition pore to protect the pore from oxidative damage. Therefore, one of the reasons why 104C1/O4C cells harboring the *hGPX-4* gene, which carries the code for the mitochondrial transfer signal of hPHGPx, were resistant to GGA-induced collapse of $\Delta\Psi m$ could be that PHGPx expressed in 104C1/O4C cells is involved in protecting ANT and/or cardiolipin in situ from peroxidative damage. We are now investigating the integrity of ANT and cardiolipin after GGA treatment in both cell lines.

PHGPx is an enzyme that catalyzes the reduction of phospholipid hydroperoxides to their hydroxy phospholipids as well as reduces hydrogen peroxide to water. The forced expression of the *hGPX-4* gene in the PHGPx-negative cells might decrease the intracellular content of the endogenously produced phospholipid hydroperoxides and hydrogen peroxide sufficiently to attenuate the peroxidative reactions. In order to illustrate the protective effect of the PHGPx enzyme against GGA treatment, it is essential for us to measure the remaining hydroperoxides level in the cells.

Next, we must discuss how GGA treatment can give rise to hyper-production of ROSs or enhanced peroxidation reactions in the cells. Many antitumor agents and apoptosis-inducing small chemicals such as arotinoids [Chun et al., 2003], paclitaxel [Andre et al., 2002], terpenoids [Tan et al., 2003], flavonoids [Shen et al., 2004], and polyphenols [Nakagawa et al., 2004] have been reported to generate ROSs during apoptosis, although these compounds have no common chemical structure or properties. The production of ROSs is commonly an early event that occurs within $15 \sim 30$ min after addition of such drugs. Inasmuch as these agents including GGA are not pro-oxidant, they should have intracellular target site(s) to generate ROSs. One of the major ROS-generating organelles is the mitochondrion. GGA-induced generation of superoxide anion radicals may be explained by impairment of the mitochondrial electron transport system. However, no evidence has been so far demonstrated for any interactions of GGA with the respiratory chain, except that GGA and CoQ_{10}, a lipid messenger for electron transport from complex I or II to complex III, have a common structural domain. In the present study, GGA induced a hyper-production of superoxide with a peak at $15 \sim 30$ min in both 104C1 and 104C1/O4C clones, suggesting that mitochondria may serve as direct targets for GGA and the generated superoxide may be converted to hydrogen peroxide by mitochondrial superoxide dismutase with the same kinetics in both cell lines. We speculate that the converted hydrogen peroxide might consequently accumulate in PHGPx-null 104C1 cells, but might be reduced to water in PHGPx-expressing 104C1/O4C cells. In fact, a significant accumulation of hydrogen peroxide was detected at 4 h after the GGA addition only in 104C1 cells (Figs. 6, 7).

In sharp contrast to 104C1 cells, 104C1/O4C cells did not accumulate hydrogen peroxide, probably because the expressed hPHGPx enzyme might convert hydrogen peroxide in situ to the inert water in mitochondria. In other words, the forced expression of the *hGPX-4* gene in the PHGPx-negative cells may decrease the intramitochondrial contents of the endogenously produced hydrogen peroxide enough to attenuate the peroxidative reactions. Recently, we found an efficient positive-cooperative catalytic

activity of recombinant hPHGPx toward cardiolipin monohydroperoxide with a Hill coefficient value of 2.33 [Shidoji et al., 2002]. The measurement of the putative cardiolipin hydroperoxide level in the cells is essential to confirm a PHGPx-based protective mechanism against GGA-induced apoptosis.

In conclusion, GGA-induced dissipation of the $\Delta\Psi m$ in guinea pig 104C1 cells and the resultant apoptotic cell death were both prevented by the constitutive expression of the antioxidant enzyme PHGPx, strongly indicating that cellular peroxides are involved in the molecular mechanism of GGA-induced apoptosis.

ACKNOWLEDGMENTS

The authors thank Dr. Luigi M. De Luca (NCI, NIH, Bethesda) for his kind advice during preparation of this manuscript.

REFERENCES

Afri M, Frimer AA, Cohen Y. 2004. Active oxygen chemistry within the liposomal bilayer. Part IV: Locating 2′,7′-dichlorofluorescein (DCF), 2′,7′-dichlorodihydrofluorescein (DCFH), and 2′,7′-dichlorodihydrofluorescein diacetate (DCFH-DA) in the lipid bilayer. Chem Phys Lipids 131:123–133.

Andre N, Carre M, Brasseur G, Pourroy B, Kovacic H, Briand C, Braguer D. 2002. Paclitaxel tarxgets mitochondria upstream of caspase activation in intact human neuroblastoma cells. FEBS Lett 532:256–260.

Araki H, Shidoji Y, Yamada Y, Moriwaki H, Muto Y. 1995. Retinoid agonist activities of synthetic geranylgeranoic acid derivatives. Biochem Biophys Res Commun 209:66–72.

Chun KH, Benbrook DM, Darrell-Berlin K, Hong WK, Lotan R. 2003. The synthetic heteroarotinoid SHetA2 induces apoptosis in squamous carcinoma cells through a receptor-independent and mitochondria-dependent pathway. Cancer Res 63:3826–3832.

Daiber A, Oelze M, August M, Wendt M, Sydow K, Wieboldt H, Kleschyov AL, Munzel T. 2004. Detection of superoxide and peroxynitrite in model systems and mitochondria by the luminol analogue L-012. Free Rad Res 38:259–269.

Duan YJ, Komura S, Fiszer-Szafarz D, Yagi K. 1988. Purification and characterization of a novel monomeric glutathione peroxidase from rat liver. J Biol Chem 263:19003–19008.

Esworthy RS, Doan K, Doroshow JH, Chu FF. 1994. Cloning and sequencing of the cDNA encoding a human testis phospholipid hydroperoxide glutathione peroxidase. Gene 144:317–318.

Giron-Calle J, Schmid H. 1996. Peroxidative modification of a membrane protein. Conformation-dependent chemical modification of adenine nucleotide translocase in Cu^{2+}/*tert*-butyl hydroperoxide treated mitochondria. Biochemistry 35:15440–15446.

Halestrap A, Woodfield K, Connern C. 1997. Oxidative stress, thiol reagents, and membrane potential modulate the mitochondrial permeability transition by affecting nucleotide binding to the adenine nucleotide translocase. J Biol Chem 272:3346–3354.

Kroemer G, Zamzami N, Susin S. 1997. Mitochondrial control of apoptosis. Immunol Today 18:44–51.

Masini A, Ceccarelli D, Trenti T, Gallesi D, Muscatello U. 1993. Mitochondrial inner membrane permeability changes induced by octadecadienoic acid hydroperoxide. Role of mitochondrial GSH pool. Biochim Biophys Acta 1101:84–89.

Muto Y, Moriwaki H, Omori M. 1981. In vitro binding affinity of novel synthetic polyprenoids (polyprenoic acids) to cellular retinoid-binding proteins. Jpn J Cancer Res 72:974–977.

Nakagawa H, Hasumi K, Woo JT, Nagai K, Wachi M. 2004. Generation of hydrogen peroxide primarily contributes to the induction of Fe(II)-dependent apoptosis in Jurkat cells by (−)-epigallocatechin gallate. Carcinogenesis 25: 1567–1574.

Nakamura N, Shidoji Y, Yamada Y, Hatakeyama H, Moriwaki H, Muto Y. 1995. Induction of apoptosis by acyclic retinoid in the human hepatoma-derived cell line, HuH-7. Biochem Biophys Res Communun 207:382–388.

Nakamura N, Shidoji Y, Moriwaki H, Muto Y. 1996. Apoptosis in human hepatoma cell line induced by 4,5-didehydro geranylgeranoic acid (acyclic retinoid) via down-regulation of transforming growth factor-alpha. Biochem Biophys Res Communun 219:100–104.

Polyak K, Xia Y, Zweier JL, Kinzler KW, Vogelstein B. 1977. A model for p53-induced apoptosis. Nature 389: 300–305.

Pushpa-Rekha TR, Burdsall AL, Oleksa LM, Chisolm GM, Driscoll DM. 1995. Rat phospholipid-hydroperoxide glutathione peroxidase. cDNA cloning and identification of multiple transcription and translation start sites. J Biol Chem 270:26993–26999.

Ritov VB, Banni S, Yalowich JC, Day BW, Claycamp HG, Corongiu FP, Kagan VE. 1996. Non-random peroxidation of different classes of membrane phospholipids in live cells detected by metabolically integrated *cis*-parinaric acid. Biochim Biophys Acta 1283:127–140.

Shen SC, Ko CH, Tseng SW, Tsai SH, Chen YC. 2004. Structurally related antitumor effects of flavanones in vitro and in vivo: Involvement of caspase 3 activation, p21 gene expression, and reactive oxygen species production. Toxicol Appl Pharmacol 197:84–95.

Shidoji Y, Ogawa H. 2004. Natural occurrence of cancer-preventive geranylgeranoic acid in medicinal herbs. J Lipid Res 45:1092–1103.

Shidoji Y, Nakamura N, Moriwaki H, Muto Y. 1997. Rapid loss in the mitochondrial membrane potential during geranylgeranoic acid-induced apoptosis. Biochem Biophys Res Communun 230:58–63.

Shidoji Y, Komura S, Ohishi N, Yagi K. 2002. Interaction between cytochrome c and oxidized mitochondrial lipids. In: Quinn PJ, Kagan VE, editors. Phospholipid metabolism in apoptosis. Subcellular biochemistry, vol. 36. New York: Kluwer Academic/Plenum Publishers. pp 19–37.

Skulachev VP. 1996. Why are mitochondria involved in apoptosis? Permeability transition pores and apoptosis as

selective mechanisms to eliminate superoxide-producing mitochondria and cell. FEBS Lett 97:7–10.

Sun Q, Kojima H, Komura S, Ohishi N, Yagi K. 1997. Effect of selenium on human phospholipid hydroperoxide glutathione proxidase expression and host cell susceptibility to lipid hydroperoxide-mediated injury. Biochem Mol Biol Int 42:957–963.

Tan Y, Yu R, Pezzuto JM. 2003. Betulinic acid-induced programmed cell death in human melanoma cells involves mitogen-activated protein kinase activation. Clin Cancer Res 9:2866–2875.

Yagi K, Komura S, Kojima H, Sun Q, Nagata N, Ohishi N, Nihikimi M. 1996. Expression of human phospholipid hydroperoxide glutathione peroxidase gene for protection of host cells from lipid hydroperoxide-mediated injury. Biochem Biophys Res Communun 219:486–491.

Yagi K, Shidoji Y, Komura S, Kojima H, Ohishi N. 1998. Dissipation of mitochondrial membrane potential by exogenous phospholipid monohydroperoxide and protection against this effect by transfection of cells with phospholipid hydroperoxide glutathione peroxidase gene. Biochem Biophys Res Communun 245:528–533.

Yamada Y, Shidoji Y, Fukutomi Y, Ishikawa T, Kaneko T, Nakagama H, Imawari M, Moriwaki H, Muto Y. 1994. Positive and negative regulations of albumin gene expression by retinoids in human hepatoma cell lines. Mol Carcinog 10:151–158.